Experimental generation of frequency-tunable entangled optical beams with continuous variables

Zhihui Yan (闫智辉), Yana Shang (商娅娜), Xiaojun Jia (贾晓军)*, and Changde Xie (谢常德)

State Key Laboratory of Quantum Optics and Quantum Optics Devices, Institute of Opto-Electronics, Shanxi University, Taiyuan 030006, China

**Corresponding author: jiaxj@sxu.edu.cn*

Received September 7, 2010; accepted October 25, 2010; posted online February 24, 2011

Frequency tunable continuous variable (CV) entangled optical beams are experimentally demonstrated from a non-degenerate optical parametric oscillator working above the threshold. The measured correlation variances of amplitude and phase quadratures are 3.2 and 1.5 dB, respectively, below the corresponding shot noise level (SNL) in the tuning range of 580 GHz (2.25 nm). The frequency tuning is realized by simply controlling the temperature of the nonlinear crystal.

OCIS codes: 270.6570, 190.4410, 190.4970, 190.4360.
doi: 10.3788/COL201109.032701.

Optical entangled states with quantum correlations of both amplitude and phase quadratures have become important resources for testing fundamental ideas of quantum physics[1,2] and developing quantum information with continuous variables (CVs)[3−5]. Optical parametric oscillators (OPOs) operated below or above the oscillation thresholds are reliable quantum systems used to produce CV optical entangled states. In most experiments on CV quantum communication and computation, OPOs below the threshold have often been used for generating Einstein-Podolsky-Rosen (EPR) entangled optical beams with degenerate frequency[2,5]. Along with the development of CV quantum information science and techniques, bright entangled optical beams are desired. In recent years, intense entangled states of light operated above the threshold have been obtained from non-degenerate OPOs (NOPOs)[6−11]. Further, to exploit CV quantum information networks, including several nodes, the frequency of the entangled light have been precisely tuned to resonate with the transition of atomic levels to interact with atomic samples[12−18]. The frequency-tunable twin beams with only intensity correlated and amplitude squeezing have been experimentally produced with NOPOs above the threshold and have been applied to frequency modulation (FM) spectroscopy[15−20]. In Ref. [21], a narrow-band frequency tunable light source of continuous quadrature entanglement, which is a frequency NOPO below threshold, has been presented, in which the signal and idler fields was separated by 740 MHz. In this letter, we present an experimental result on the generation of frequency-tunable optical fields with CV entanglement at 1080 nm. Given that the selected nonlinear crystal, $KTiOPO_4$ (KTP), has broader phase matching temperature, the frequency-tunable entangled optical beams are achieved by simply tuning the temperature of the crystal placed in an OPO above the threshold. The measured amplitude-difference and phase-sum correlation variances at 2 MHz are 3.2 and 1.5 dB, respectively, below the corresponding shot noise level (SNL) in the tuning range of 580 GHz (2.25 nm).

For a NOPO consisting of a second-order non-linear crystal inside an optical cavity, the frequency of pump laser (ω_0) and the frequencies of the generated signal and idler optical beams (ω_1 and ω_2) fulfill the energy conservation expressed by $\omega_0 = \omega_1 + \omega_2$. The correlation variances of amplitude ($\hat{X}$) and phase ($\hat{Y}$) quadratures between the output signal and idler beams from the NOPO operating above the oscillation threshold are expressed by[8,22]

$$V\ \hat{X}_- = S_0\left[1 - \frac{\eta\zeta^2\xi}{1+(f/B)^2}\right], \tag{1}$$

$$V\ \hat{Y}_+ = S_0\left[1 - \frac{\eta\zeta^2\xi}{\sigma^2+(f/B)^2}\right], \tag{2}$$

where $\hat{X}_- = \hat{X}_1 - \hat{X}_2$ and $\hat{Y}_+ = \hat{Y}_1 + \hat{Y}_2$, in which ($\hat{X}_1$,$\hat{Y}_1$) and ($\hat{X}_2$,$\hat{Y}_2$) are the quadrature amplitude and quadrature phase of the signal (idler) beams, respectively. In addition, $f = \Omega/2\pi$ is the noise frequency; S_0 is the SNL; B and ξ are cavity bandwidth and the output coupling efficiency of NOPO, respectively; ζ is the transmission efficiency of Mach-Zehnder (M-Z) interferometer used for measuring the correlation variances; η is the detector efficiency of photo-diodes; $\sigma = (P/P_0)^{1/2}$ is the pump parameter, in which P is the pump power and P_0 is the threshold pump power of the NOPO.

The experimental setup is depicted in Fig. 1, which shows that the frequency tunable entangled optical beams are generated from a NOPO working above the threshold, which is pumped by an intracavity frequency-doubling Nd:YAP/KTP laser (YuGuang Company F-IVB). The second-harmonic wave at 540 nm from the laser serves as the pump field (ω_0) of the NOPO. In this experiment, the NOPO cavity consisted of a 10-mm-long α-cut type-II non-critical phase matched KTP crystal, and a concave mirror M0 with a 50-mm radius of curvature was mounted upon a piezoelectric transducer (PZT) to lock the cavity length on resonance with the pump laser using the Pound-Drever-Hall FM technique. One end face of the crystal was coated with high reflection

 © 2011 Chinese Optics Letters

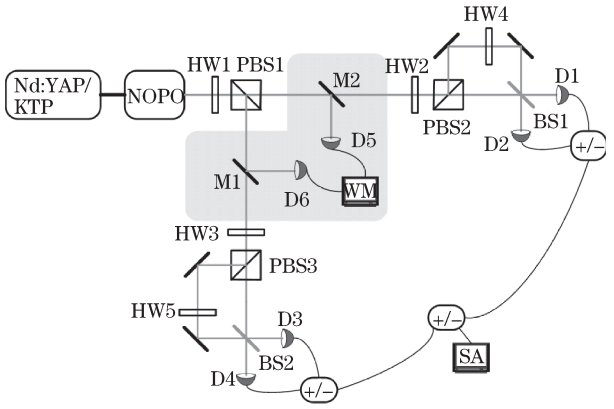

Fig. 1. Schematic diagram of the experimental setup. D1−4: ETX500 InGaAs photodiode detectors; D5−6: input port of wavelength meter; SA: spectrum analyzer.

(HR) at 1080 nm and a transmission of 39% at 540 nm, which was used for the input mirror of the NOPO, while the other end face was coated with anti-reflection (AR) at both 1080 and 540 nm. The output fields were extracted from a concave mirror with HR at 540 nm and a transmission of 3.2% at 1080 nm. The NOPO was triply resonant for the signal, idler, and pump beam. The finesses for the pump and signal (idler) light were 17 and 165, respectively. In this case, many pairs of the signal and idler modes with different frequencies were produced within the wide resonant peak of the intracavity pump field under the phase matching condition for the parametric down conversion. By tuning the temperature of the KTP crystal, the entangled optical beams with different frequencies were generated, and triple resonance was achieved within the full-width at half-maximum of the smooth resonant peak of the pump field[5,6]. In this letter, the output beams were separated by a polarizing-beam-splitter (PBS1) and were detected by two sets of unbalanced M-Z interferometer, respectively. The five half-wave plates HW1-5 were used for the polarization alignment, and the two movable mirrors M1 and M2 were used to switch the measurement of the wavelength or the correlation noise of the output beam from the NOPO.

Glockl *et al.*[23] presented an elegant scheme allowing us to perform the subshot-noise measurements of the phase and amplitude quadratures of a bright optical beam as well as the corresponding SNL experimentally using a set of M-Z interferometer with unbalanced arm lengths, instead of using a separate local oscillator. For measuring the fluctuation of the phase quadratures and the corresponding SNL of the mode $a_1(a_2)$, the polarization of HW2 (HW3) were rotated to a specified direction to allow the beam $a_1(a_2)$ to perform 50% transmission through PBS2 (PBS3), and then the PBS2 (PBS3) serves as the input beam-splitters of the interferometers. When the relative optical phase shift (φ) between two optical fields passing through the short and long arms is adjusted to $\varphi = \pi/2 + 2k\pi$ (k is an integer), and at the same time the phase shift (θ) of the spectral component of radio frequency fluctuations at a sideband frequency ($\Omega = 2\pi f$) is controlled to $\theta = \pi$, the beam-splitter BS1 (BS2) of 50% becomes the output coupler of the interferometer; as a result, the output beams are detected by the photodiodes D1 and D2 (D3 and D4), and the difference and the sum of the ac photocurrents may be used to evaluate the fluctuation of the phase quadratures and the SNL of the input mode a1(a2), respectively. Therefore, to measure the phase fluctuation of the input field, one should take the difference in length ΔL between the short and the long arms as $\Delta L = c\pi/(n\Omega)$ (where c is the speed of light, and n is the refraction index of the transmission medium) in order to meet the condition $\theta = n\Omega\Delta L/c = \pi$. For measuring at $f = 2$ MHz the length difference ΔL between the long and short arms of the unbalanced M-Z interferometer consisting of the optical fiber should be 48 m. To ensure the stability of the M-Z interferometer with such a large length difference between the two arms, we used two sets of optical fibers as the long and short arms. Both the total length and the length difference ΔL of the interferometer were exactly fixed by the length of the chosen fiber for each arm. For locking the optical phase, a PZT was mounted on one of the mirrors of the M-Z interferometer to adjust the optical paths precisely with the electronic error signals, which were obtained from the difference of the direct current (DC) photocurrents detected by a pair of photodiodes D1 and D2 (D3 and D4). The error signals were then fed back to the PZT to maintain actively the required phase difference of $\pi/2 + 2k\pi$. The phase locking error of the system was about $(\pi/2 \pm \pi/36) + 2k\pi$[24]. When the polarization of HW2 (HW3) was rotated to another specified direction to allow the beam $a_1(a_2)$ to totally transmit from PBS2 (PBS3) and arrive at BS1 (BS2) only through the short arm of the interferometer, the sum and the difference photocurrents were then used to evaluate the fluctuation of the amplitude quadratures and the SNL of the input mode $a_1(a_2)$, respectively.

When the two movable mirrors M1 and M2 of 100% reflectivity were moved in one of the light beams, the reflected beams from each mirror were injected to the input port of wavelength meter (WM) in order to measure their respective frequencies. When the frequencies of the output signal and idler beam were nearly degenerate, we measured the frequency difference between the two with beating signal by another interferometer (not shown in the figure).

Given that the α-cut KTP crystal used in our system has a broad, full temperature-width from about 40 °C to around 63 °C for achieving the type-II noncritical phase matching, we can tune the frequencies of entangled light beams by changing the temperature of KTP placed in an electronic temperature-controlled oven. Figure 2 shows the change of the wavelengths of the output signal and idler beams from the NOPO when the temperature of KTP crystal is tuned. The solid lines indicate the ideal phase matching condition. The tunable temperature range of $43 - 80$ °C is limited by the home-made oven. The frequency of the signal (idler) beam can be changed from 1079.490 to 1081.739 nm (or from 1080.437 to 1078.188 nm) continuously. The tunable wavelength range is about 2.25 nm, and the maximal wavelength difference between signal and idler beams reaches up to 3.55 nm, which corresponds to a frequency range of 910 GHz. The agreement between the theoretical calculation and experimental measurement, on one hand, and

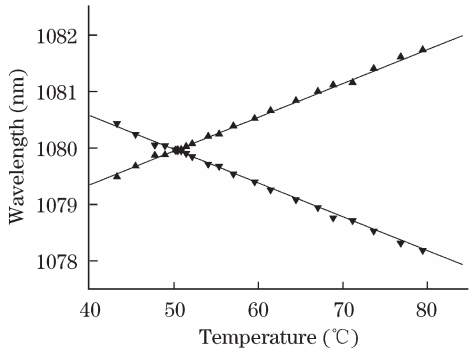

Fig. 2. Wavelengths of the output signal and idler beams from the NOPO changing with the temperature of the KTP crystal. The solid line is the calculated curve; ▲ and ▼ are the measured wavelengths of the signal and idler beams, respectively.

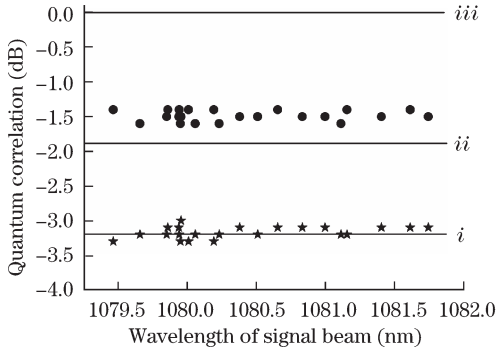

Fig. 3. Measured noise power of the twin beams at 2 MHz dependent on the wavelength of signal beam. *i* is the calculated value of amplitude correlation variance, *ii* is the calculated value of phase anticorrelation variance, *iii* is the SNL, ⋆ is the measured amplitude correlation variances, • is the measured phase anti-correlation variances.

the linearity of the wavelength temperature function on the other show that the NOPO can be used as a good tunable device. When the frequencies of output beams are nearly degenerate, the measured minimum frequency difference is only 0.87 MHz, which has been obtained by measuring the beating signal of signal and idler beams.

We measured the quantum noise spectra of the output beams by removing M1 and M2 and rotating the polarization of HW2 and HW3 to a specified direction. Subtracting (adding) the two photocurrents of the amplitude (phase) quadratures respectively measured by each M-Z interferometer with a negative (positive) power combiner $(+/-)$, we then obtained the correlation (anticorrelation) variances $V\hat{X}_-$ $(V\hat{Y}_+)$ of the amplitude (phase) quadratures between the output light beams. The functions of the measured amplitude and phase correlation variances versus different wavelengths of the output signal beam are shown in Fig. 3. The measured $V\hat{X}_-$ (⋆) and $V\hat{Y}_+$ (•) are 3.2 ± 0.1 and $1.5\pm$ 0.1 dB below the normalized SNL (0 dB), respectively, and the correlations were almost kept constant in the tuning range. These results are in reasonable agreement with the calculated results (solid line) according to Eqs. (1) and (2) using the parameters of our experimental system: $\eta = 90\%, \zeta = 81\%, \xi = 88\%$, $\sigma = (195\ \text{mW}/130\ \text{mW})^{1/2} = 1.22$, $B = 15.4$ MHz, and $f = 2$ MHz. In the measurements of the correlation variances (Fig. 3) we use the normalized SNL ($S_0 = 1$, line *iii* in Fig. 3). The measured amplitude correlation variances match perfectly with the calculated result from Eq. (1) (line *i*). However, the measured phase correlation variances are higher by 0.3 dB than that under the theoretical calculation; this is because the worse mode-matching efficiencies and the influences of the excess and spurious phase noises in the pump field have not been involved in the calculation using Eq. 2 (line *ii*). The complicated factors influencing the phase correlation of twin beams have been analyzed in detail in Refs. [25] and [26]. When the temperature of the KTP crystal is below 43 °C, the measured correlation variances of both the quadrature amplitude and quadrature phases drop quickly due to the fact that the temperature has gone out of the phase-matching range of the KTP crystal. The measured value of $(V\hat{X}_- + V\hat{Y}_+)$ is given by

$$V\hat{X}_- + V\hat{Y}_+ = 1.19 < 2, \tag{3}$$

which satisfies the criterion of CV quantum entanglement[27,28].

In conclusion, frequency tunable entangled optical beams are produced from a NOPO operated above the threshold. The measured correlation variances of amplitude and phase quadratures are 3.2± 0.1 and 1.5±0.1 dB below the corresponding SNL within a tuning range of 2.25 nm. The tunable range can be extended if the temperature range for phase matching in nonlinear crystal is increased. A simple scheme for producing frequency-tunable entangled optical beams is provided. In choosing appropriate pump lasers and nonlinear crystals, it is possible to obtain the tunable entangled optical beams at any desired frequency regions using the presented scheme. The wavelength of 1080 nm is close to the transitions of Li (1079.218 nm), Ba (1079.094 nm), and He (1082.909 nm) atoms; thus the produced entangled light might find direct applications in studying the interaction of light and matter as well as quantum information based on these atoms.

This work was supported by the National Natural Science Foundation of China (Nos. 60736040 and 11074157), the NSFC Project for Excellent Research Team (No. 60821004), and the National Basic Research Program of China (No. 2010CB923103).

References

1. A. Aspect, P. Grangier, and G. Roger, Phys. Rev. Lett. **47,** 460 (1981).
2. Z. Y. Ou, S. F. Pereira, H. J. Kimble, and K. C. Peng, Phys. Rev. Lett. **68,** 3663 (1992).
3. S. L. Braunstein and P. van Loock, Rev. Mod. Phys. **77,** 513 (2005).
4. A. Furusawa, J. L. Sorensen, S. L. Braunstein, C. A. Fuchs, H. J. Kimble, and E. S. Polzik, Science **282,** 706 (1998).
5. X. Li, Q. Pan, J. Jing, J. Zhang, C. Xie, and K. Peng, Phys. Rev. Lett. **88,** 047904 (2002).
6. M. D. Reid and P. D. Drummond, Phys. Rev. Lett. **60,** 2731 (1988).

7. A. S. Villar, L. S. Cruz, K. N. Cassemiro, M. Martinelli, and P. Nussenzveig, Phys. Rev. Lett. **95,** 243603 (2005).
8. X. Su, A. Tan, X. Jia, Q. Pan, C. Xie, and K. Peng, Opt. Lett. **31,** 1133 (2006).
9. J. Jing, S. Feng, R. Bloomer, and O. Pfister, Phys. Rev. A **74,** 041804 (2006).
10. G. Keller, V. D'Auria, N. Treps, T. Coudreau, J. Laurat, and C. Fabre, Opt. Express **16,** 9351 (2008).
11. A. S. Coelho, F. A. S. Barbosa, K. N. Cassemiro, A. S. Villar, M. Martinelli, and P. Nussenzveig, Science **326,** 823 (2009).
12. B. Julsgaard, J. Sherson, J. I. Cirac, J. Fiurasek, and E. S. Polzik, Nature **432,** 482 (2004).
13. J. Appel, E. Figueroa, D. Korystov, M. Lobino, and A. I. Lvovsky, Phys. Rev. Lett. **100,** 093602 (2008).
14. K. Honda, D. Akamatsu, M. Arikawa, Y. Yokoi, K. Akiba, S. Nagatsuka, T. Tanimura, A. Furusawa, and M. Kozuma, Phys. Rev. Lett. **100,** 093601 (2008).
15. G. M. Gibson, M. H. Dunn, and M. J. Padgett, Opt. Lett. **23,** 40 (1998).
16. H. B. Wang, Z. H. Zhai, S. K. Wang, and J. R. Gao, Europhys. Lett. **64,** 15 (2003).
17. S. Kasapi, S. Lathi, and Y. Yamamoto, Opt. Lett. **22,** 478 (1997).
18. F. Marin, A. Bramati, V. Jost, and E. Giacobino, Opt. Commun. **140,** 146 (1997).
19. M. E. Klein, C. K. Laue, D. H. Lee, K. J. Boller, and R. Wallenstein, Opt. Lett. **25,** 490 (2000).
20. A. Porzio, C. Altucci, M. Autiero, C. Delisio, and S. Solimeno, Appl. Phys. B **73,** 763 (2001).
21. C. Schori, J. L. Sorensen, and E. S. Polzik, Phys. Rev. A **66,** 033802 (2002).
22. C. Fabre, E. Giacobino, A. Heidmann, and S. Reynaud, J. Phys. **50,** 1209 (1989).
23. O. Glockl, U. L. Andersen, S. Lorenz, Ch. Silberhorn, N. Korolkova, and G. Leuchs, Opt. Lett. **29,** 1936 (2004).
24. Y. Wang, H. Shen, X. Jin, X. Su, C. Xie, and K. Peng, Opt. Express **18,** 6149 (2010).
25. D. Wang, Y. Shang, X. Jia, C. Xie, and K. Peng, J. Phys. B: At. Mod. Opt. Phys. **41,** 035502 (2008).
26. A. S. Villar, K. N. Cassemiro, K. Dechoum, A. Z. Khonry, M. Martinelli, and P. Nussenzveig, J. Opt. Soc. Am. B **24,** 249 (2007).
27. L.-M Duan, G. Giedke, J. I. Cirac, and P. Zoller, Phys. Rev. Lett. **84,** 2722 (2000).
28. R. Simon, Phys. Rev. Lett. **84,** 2726 (2000).